

1-5-2010

Homozygous Frameshift Mutation in TMCO1 Causes A Syndrome with Craniofacial Dysmorphism, Skeletal Anomalies, and Mental Retardation

Baozhong Xin
DDC Clinic for Special Needs Children

Erik G. Puffenberger
The Clinic for Special Children

Susan Turben
DDC Clinic for Special Needs Children

Haiyan Tan
Cleveland State University

Aimin Zhou
Cleveland State University, A.ZHOU@csuohio.edu

Follow this and additional works at: https://engagedscholarship.csuohio.edu/scichem_facpub

 Part of the [Chemistry Commons](#)

How does access to this work benefit you? Let us know!

Recommended Citation

Xin, Baozhong; Puffenberger, Erik G.; Turben, Susan; Tan, Haiyan; Zhou, Aimin; and Wang, Heng, "Homozygous Frameshift Mutation in TMCO1 Causes A Syndrome with Craniofacial Dysmorphism, Skeletal Anomalies, and Mental Retardation" (2010). *Chemistry Faculty Publications*. 391.
https://engagedscholarship.csuohio.edu/scichem_facpub/391

This Article is brought to you for free and open access by the Chemistry Department at EngagedScholarship@CSU. It has been accepted for inclusion in Chemistry Faculty Publications by an authorized administrator of EngagedScholarship@CSU. For more information, please contact library.es@csuohio.edu.

Authors

Baozhong Xin, Erik G. Puffenberger, Susan Turben, Haiyan Tan, Aimin Zhou, and Heng Wang

Homozygous frameshift mutation in *TMCO1* causes a syndrome with craniofacial dysmorphism, skeletal anomalies, and mental retardation

Baozhong Xin , Erik G. Puffenberger , Susan Turben , Haiyan Tan , Aimin Zhou , and Heng Wang

We identified an autosomal recessive condition in 11 individuals in the Old Order Amish of northeastern Ohio. The syndrome was characterized by distinctive craniofacial dysmorphism, skeletal anomalies, and mental retardation. The typical craniofacial dysmorphism included brachycephaly, highly arched bushy eyebrows, synophrys, long eyelashes, low-set ears, microdontism of primary teeth, and generalized gingival hyperplasia, whereas Sprengel deformity of scapula, fusion of spine, rib abnormalities, pectus excavatum, and pes planus represented skeletal anomalies. The genome-wide homozygosity mapping using six affected individuals localized the disease gene to a 3.3-Mb region on chromosome 1q23.3-q24.1. Candidate gene sequencing identified a homozygous frameshift mutation, c.139 140delAG, in the transmembrane and coiled-coil domains 1 (*TMCO1*) gene, as the pathogenic change in all affected members of the extended pedigree. This mutation is predicted to result in a severely truncated protein (p.Ser47Ter) of only one-fourth the original length. The *TMCO1* gene product is a member of DUF841 superfamily of several eukaryotic proteins with unknown function. The gene has highly conserved amino acid sequence and is universally expressed in all human tissues examined. The high degree of conservation and the ubiquitous expression pattern in human adult and fetal tissues suggest a critical role for *TMCO1*. This report shows a *TMCO1* sequence variant being associated with a genetic disorder in human. We propose "TMCO1 defect syndrome" as the name of this condition.

Amish | transmembrane and coiled coil domains 1 gene | genotyping and mapping | homozygosity | SNP arrays

Although there are a significant number of autosomal phenotypes associated with syndromic and nonsyndromic mental retardation, the identification of these genes has been relatively slow, and the underlying pathophysiology of mental retardation remains unexplained in most cases (1). The use of homozygosity mapping in consanguineous families and isolated populations is a powerful tool for revealing genetic lesions in various recessive conditions (2-6). Yet, this approach, as with conventional linkage mapping, requires that the clinical phenotype be well defined and easily recognizable. Unfortunately, mental retardation as a clinical descriptor is nonspecific unless found in association with other features. Here, we describe a unique genetic condition characterized by craniofacial dysmorphism, skeletal anomalies, and mental retardation in the Old Order Amish of northeastern Ohio. Through a genome wide mapping study, we localized the disease gene to chromosome 1q23.3-q24.1 and identified a homozygous frameshift mutation in the transmembrane and coiled coil domains 1 gene (*TMCO1*) as the cause of this autosomal recessive condition, thus we propose "TMCO1 defect syndrome" as the name for this disease.

Results

Clinical Phenotype. TMCO1 defect syndrome was diagnosed in 11 individuals (6 males, 5 females) ranging in age from 3 to 39 years. All 11 patients demonstrated Old Order Amish ancestry, and genealogical analyses revealed multiple lines of common descent between all parents of affected children (Fig. 1). The phenotype was not observed in the parents or 23 unaffected siblings.

A history of first trimester spontaneous abortions was reported by four mothers with an overall incidence of 10 of 45 pregnancies (22%). The abnormalities in affected individuals were observed from prenatal period (Table 1). Ventriculomegaly, cleft lip and palate were noted through prenatal ultrasound in one patient, although this procedure was not routinely performed in this ethnic group. All affected individuals were born with normal birth weight for their gestational age (10 of 11 being full term), and five exhibited length exceeding the 90th percentile. Nine infants were reportedly macrocephalic at birth, probably secondary to their dysmorphic craniofacial features because their occipitofrontal circumference in fact was not significantly increased (range 3-95%, average 33%) (Table 1 and Table 2). Hypotonia and poor feeding were found in all newborns. Routine hematology and metabolic assays were generally within normal ranges. The standard karyotype analysis was performed on at least four patients and reported as normal.

The craniofacial dysmorphism was noticeable at birth and included brachycephaly, flat face, low hairline, low set ears, high arched palate, and cleft lip and palate. Other characteristic dysmorphic features, such as highly arched bushy eyebrows, synophrys, orbital hypertelorism, long eyelashes, wide nose bridge, short nose with anteverted nares, and microdontism of primary teeth appeared later, generally before they reached preschool age. Generalized gingival hyperplasia usually appeared after the eruption of permanent teeth (Fig. 2, Fig. S1, and Table 1).

Skeletal dysmorphism, such as pectus excavatum and club feet, was noted during early infancy, whereas scoliosis and long, hyperextensible fingers developed when the patients reached puberty. Fusion of the cervical or thoracic spine, rib anomalies (including fusion, hypoplasia, or broad or missing ribs), and Sprengel deformity of scapula, were usually incidental findings during routine imaging studies for other purposes. The actual incidence of these abnormalities in TMCO1 defect syndrome

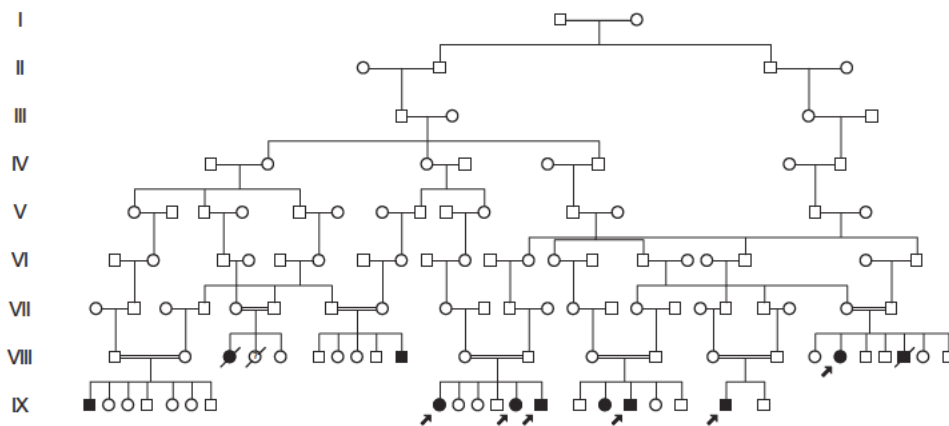


Fig. 1. Partial pedigree of the family with *TMC01* defect syndrome. Filled symbols represent affected individuals, and open symbols represent unaffected individuals. Circles and squares denote females and males, respectively. A double line identifies consanguinity. Arrows indicate affected individuals included in genetic mapping study and sequence analysis.

might be higher if systematic osseous surveys were performed in all patients (Table 1, Table 2, Fig. 2, and Fig. S1). The skeletal anomalies found in this condition mostly involve the axial skeleton, which embryologically originates from somites. There was significant divergence in patients' stature, two of them having tall stature with height >95th percentile, whereas three exhibited short stature with height in less than the 3rd percentile. Global developmental delay was found in all affected individuals, although regression was not observed.

Neurological examination revealed depressed deep tendon reflexes and unstable gait, and intention tremor developed in some older patients. Imaging studies demonstrated mild prominence of ventricles viewed through CT or MRI (Fig. 2H). Sluggish speech with a loud and hoarse voice was found in all verbal patients. Anatomical abnormalities of the genitourinary system were noted, including renal agenesis, hydronephrosis, vesicoureteral reflux, hypoplastic labia minora, hydrocele, and undescended testes. Other clinical features with high incidence were frequent otitis media, sinusitis, strabismus, and constipation although they were less specific (Table 1).

Genotyping and Mapping. To determine the genetic basis of this syndrome, we performed a genome wide homozygosity mapping study by using Affymetrix GeneChip Mapping 10K SNP Arrays with six affected individuals from this large consanguineous pedigree (Fig. 1). A single large, shared block of homozygous SNPs was identified on chromosome 1q23.3 q24.1 in all six patients (Fig. 3). The homozygous segment contained 17 contiguous SNPs and spanned 3.3 Mb. Examination of the minimal shared region, which was flanked by SNPs rs1396550 and rs1372685, revealed 23 known or predicted genes based on both the NCBI and Celera annotations.

Mutation Identification and mRNA Analysis. For each gene within the mapped interval, we assessed function and expression to generate a priority list for sequencing. Candidate gene sequencing was performed to screen the coding region and associated intronic splice junctions by using genomic DNA from one patient. We sequenced six genes before we identified a homozygous 2 base pair deletion (c.139_140delAG) within exon 2 of the *TMC01* gene (Fig. 4A). This frameshift variant is predicted to result in premature truncation of translation at amino acid position 47 (p.Ser47Ter, Fig. 4B). Targeted sequencing of *TMC01* exon 2 revealed that all affected individuals ($n = 9$) were homozygous for the mutation, their parents were heterozygous, and no unaffected siblings were homozygous for the change. We next screened 145 ethnically matched control samples from the same geographic area where the patients were found ($n = 290$ chromosomes) and determined that none were homozygous, whereas one was het

erozygous for the c.139_140delAG mutation (estimated carrier frequency of 0.7%).

To determine the distribution of the *TMC01* mutation in other Amish populations, we screened 75 Old Order Amish from southeastern Pennsylvania for c.139_140delAG mutation. This sample included normal controls and undiagnosed patients. We found five c.139_140delAG heterozygotes for an estimated carrier frequency of 6.6%. Surprisingly, among the undiagnosed patients, we identified a single mutation homozygote. Review of his clinical history revealed a phenotype strikingly similar to the affected children from Ohio. Further testing of undiagnosed children at the Clinic for Special Children identified a total of five affected c.139_140delAG homozygotes. Review of the SNP genotype data generated previously showed that all five patients from Pennsylvania were indeed homozygous for SNPs spanning the *TMC01* locus, but the haplotypes were different (Fig. 3B). The three homozygotes from the Lancaster County Amish settlement were homozygous for a different background haplotype than the other two homozygotes, who lived in Somerset County of Pennsylvania. The Somerset County Amish haplotype matched the Ohio Amish haplotype.

To determine the mRNA expression pattern of *TMC01*, human adult and fetal multiple tissue cDNA (MTC) panels were used as templates for PCR analysis. Amplification of first strand cDNA showed ubiquitous expression in all 16 adult and 8 fetal tissues along with the control gene *GAPDH* (Fig. S2), with relatively higher level in the tissues of adult thymus, prostate, and testis.

Discussion

We describe here a unique autosomal recessive condition characterized by craniofacial dysmorphism, skeletal anomalies, and mental retardation in the Old Order Amish. The clinical features of this condition overlap with several previously defined syndromes such as Cornelia de Lange syndrome, chromosome 3q duplication, Smith Magenis syndrome, and Klippel Feil syndrome, although it is clearly distinct from these syndromes. This condition also shares numerous clinical features with some lysosomal storage diseases, but the disease does not progress as do the storage diseases. Because of the tall stature in several patients, the condition has been suspected as a Marfan like syndrome or Sotos like syndrome as well. It is obvious that the phenotype of this condition is fairly heterogeneous and the clinical diagnosis of the disease may be challenging, particularly before the phenotype is well documented. The unique position as a primary care facility has given us the opportunities to carefully and continually observe these patients in the description of the phenotype while we provide medical services. The value of accessible, continuous, and comprehensive care provided by such a clinic for affected

Table 1. Clinical features of 11 patients with *TMCO1* defect syndrome

Features	Incidence or average age
Prenatal and neonatal	
Polyhydramnios	36% (4/11)
Decreased fetal movements	36% (4/11)
Macrocephalic appearance	90% (9/10)
Hypotonia	100% (11/11)
Poor feeding	100% (11/11)
Craniofacial	
Brachycephaly and flat face	100% (11/11)
Low hairline	100% (11/11)
Low set ears	100% (11/11)
Highly arched bushy eyebrows	100% (11/11)
Synophrys	100% (11/11)
Orbital hypertelorism	100% (11/11)
Long eyelashes	100% (11/11)
Wide nose bridge	100% (11/11)
Short nose with antverted nares	100% (11/11)
Oral and dental	
High arched palate	100% (11/11)
Cleft lip and palate	27% (3/11)
Age of primary tooth eruption	15 months (8-24)
Microdontism of primary teeth	100% (9/9)
Generalized gingival hyperplasia	100% (8/8)
Skeletal	
Craniosynostosis	18% (2/11)
Fusion of spine	55% (6/11)
Short neck	55% (6/11)
Scoliosis	64% (7/11)
Sprengel deformity of scapula	80% (8/10)
Pectus excavatum	82% (9/11)
Rib anomalies	55% (6/11)
Long and hyperextensible fingers	55% (6/11)
Pes planus	100% (11/11)
Club feet	27% (3/11)
Developmental	
Roll over	11 months (5-24)
Sit up	19 months (11-36)
Walk	36 months (18-60)
Talk	33 months (16-48)
Neurological	
Unstable gait	100% (9/9)
Intention tremor	55% (6/11)
Depressed deep tendon reflexes	90% (9/10)
Prominence of ventricles viewed through CT or MRI	57% (4/7)
Psychosocial	
Mental retardation with an average full scale IQ	56 (51-61)
Nonverbal	45% (5/11)
Sluggish speech with hoarse and loud voice	100% (6/6)
Anxiety	64% (7/11)
Feed themselves	100% (10/10)
Dress themselves	75% (6/8)
Toilet training	75% (6/8)
Others	
Genital urinary tract abnormalities	45% (5/11)
Strabismus	45% (5/11)
Frequent otitis media	73% (8/11)
Frequent sinusitis	82% (9/11)
Mild hypertrichosis	64% (7/11)
Constipation	64% (7/11)

Incidence is expressed as a percentage with the number of patients applied in parentheses. The numbers in parentheses behind average age are ranges.

children has been well demonstrated in a similar clinic previously (6). We anticipate that the current work and future translational research of this condition will not only further enhance our cost effective medical services for these patients, but also provide an opportunity for early diagnosis through newborn screening and adequate genetic counseling for the high risk families.

Through genome wide homozygosity mapping and mutational analysis in affected individuals from a consanguineous pedigree, we have identified a pathogenic sequence variant, c.139_140delAG, in the *TMCO1* gene, which is associated with the disease. This alteration has not been reported as a polymorphic variant in GenBank. It cosegregates consistently with the disease phenotype, because all affected individuals are homozygous, their parents are heterozygous, and no unaffected siblings or normal controls are homozygous for the mutation. We therefore designate this condition as *TMCO1* defect syndrome.

Ten of the eleven patients initially identified are from the Geauga County settlement of Ohio. One patient from Kentucky is closely related to the individuals from this settlement. The Geauga County Amish settlement originated around 1886, with initial immigrants from Holmes County, Ohio. Amish from Pennsylvania settlements later joined them, making the Geauga settlement the fourth largest Amish community with an extant population of $\approx 15,000$. Although the history of this settlement is relatively short, genetic disorders are fairly common in the community. The carrier frequency (0.7%) is substantially lower than several other conditions recently identified in the Geauga settlement, such as hypertrophic cardiomyopathy and Charcot Marie Tooth disease (4, 5).

The identification of *TMCO1* defect syndrome patients in the Amish populations of Pennsylvania was unexpected. Targeted sequencing of *TMCO1* exon 2 for undiagnosed patients revealed five cases within two distinct Amish demes in Pennsylvania. Although several were suspected to share the same disorder, homozygosity mapping was hampered by haplotype heterogeneity. The shared haplotype for the Lancaster Amish (samples 18060, 15963, and 23235) is significantly different from the haplotype for the Somerset County, PA, and Geauga County, OH, Amish. This disparity might reflect unfortunate ancestral recombinants very near the disease gene or discrete ancestors whose genealogical ties predate emigration to the United States.

This report shows a *TMCO1* sequence variant being associated with an adverse phenotype in human. The *TMCO1* gene consists of seven coding exons, and the 564 bp coding region encodes a predicted protein of 188 amino acids. SMART sequence analysis predicted two transmembrane segments (amino acids 10-31 for TM1 and amino acids 90-109 for TM2) and a coiled coil domain (amino acids 32-89) (Fig. 4B). In addition, three phosphorylation sites (phosphoserines) involved in the signaling networks across the cell cycle were verified in the previous studies (7-10) (Fig. 4B). It is predicated that the c.139_140delAG mutation would result in a severely truncated protein lacking the second transmembrane domain, the coiled coil domain, and three potential phosphorylation sites if it escapes nonsense mediated mRNA decay. The phosphorylation sites are essential for protein function through mediation of protein-protein interactions and signal transduction.

The function of *TMCO1* is unknown. An earlier study with a GFP tagged fusion protein suggested that HP10122, an alias for *TMCO1*, was localized in the endoplasmic reticulum and Golgi apparatus (11), whereas the most recent study using the similar approach with the porcine *TMCO1* showed mitochondrial localization (12). Both groups have also investigated the expression patterns of *TMCO1* transcript in different tissues and revealed universal expression in all tissues examined, which is consistent with our results (Fig. S2). The EST Profile Viewer of the NCBI database (UniGene Hs.31498) confirms expression of *TMCO1* transcript in 42 of 45 adult tissues, including all tissue types

Table 2. Additional clinical features in individual patients with *TMCO1* defect syndrome

Patient	Age, yr	Wt at birth	Length at birth	OFC at birth	Wt at examination	Ht at examination	Additional clinical information
VII 3	28	3.884 (85%)	55.9 (99%)	N/A	N/A	157 (18%)	Fusion of thoracic spine and fused ribs (detailed unknown), died from sudden death at age of 28.
VII 10	30	3.091 (22%)	53.3 (90%)	N/A	79.4 (78%)	180 (69%)	Fusion of thoracic spine, missing ribs, hydrocele, undescended right testis, optic nerve atrophy.
VII 18	39	3.487 (57%)	48.3 (34%)	N/A	101.5 (99%)	163 (50%)	Short neck with fusion of C2 to C4 spine, obsessive compulsive tendencies, depression.
VII 21	28	4.167 (90%)	56.5 (99%)	N/A	36.4 (<1%)	157.5 (<1%)	Cervical spine fusion, rib deformities, hiatal hernia, right kidney and adrenal gland agenesis, died from spontaneous intestinal perforation and its complications at age of 28.
VIII 1	16	3.232 (29%)	48.3 (26%)	N/A	27.8 (<1%)	143 (<1%)	Hydrocele, grade II vesicoureteral reflux, calyceal diverticulum, cyst in upper pole of left kidney.
VIII 8	12	3.317 (43%)	53.3 (93%)	33.5 (22%)	52.6 (86%)	154 (67%)	Bilateral asymmetry of ribs, attention deficit hyperactivity disorder.
VIII 12	5	3.430 (95%)	44.5 (20%)	35.5 (95%)	20.4 (92%)	102 (40%)	T2 to T5 spine fusion, broad or irregular ribs, partial fusion of ribs (4, 5 and 6) bilaterally, ventricular septal defect, right aortic arch, hypoplastic pituitary gland with hypopituitarism, absent infundibulum and ectopic posterior pituitary gland, left ear sensorineural hearing loss.
VIII 13	3	3.317 (35%)	49.5 (43%)	36 (54%)	11.2 (3%)	84 (1%)	C7 to T5 spine fusion, multiple bifid ribs (3, 4 and 5), hypoplastic fourth rib and partial fusion of fifth rib, mild hydronephrosis within left kidney and right kidney agenesis, bladder diverticulum, left vesicoureteral reflux, left hydrocele, undescended right testis.
VIII 15	20	3.147 (31%)	49.5 (54%)	32 (3%)	74.4 (89%)	175 (96%)	Calcaneal valgus, obsessive compulsive tendencies, depression.
VIII 16	18	4.139 (89%)	54.6 (96%)	34 (19%)	64.4 (42%)	189 (96%)	
VIII 19	5	2.722 (9%)	50.2 (53%)	32.5 (7%)	15.9 (29%)	109 (85%)	

Weight (Wt) at birth and at examination is expressed in kilograms, and the length and head circumference (OFC) are expressed in centimeters. The numbers in parentheses are percentiles in reference to the respective age. N/A, data are not available.

tested by RT PCR for this study. Moreover, mRNA expression was also noted at all developmental stages listed from embryo to adult (<http://www.ncbi.nlm.nih.gov/UniGene/ESTProfileViewer.cgi?uglist=Hs.31498>). Amino acid sequence comparison shows the entire sequence is highly conserved among multiple species, with 100% homology among eight mammalian *TMCO1* orthologs in GenBank (Fig. S3). The extremely high degree of conservation of *TMCO1* and the ubiquitous expression pattern in human adult and fetal tissues suggest a critical role for *TMCO1*. This speculation is supported by multiple system and organ involvement in affected individuals. The complicated pregnancy in affected individuals and high incidence of first trimester spontaneous abortions observed in these families suggests a critical role for *TMCO1* in early fetal growth and development.

Materials and Methods

Subjects and Clinical Assessment. The study was approved by DDC Clinic for Special Needs Children (DDC Clinic) Institutional Review Board, and written informed consent was obtained from each participant or their legal guardian. The phenotype information was based on clinic data from 11 affected individuals, 10 of them were from Ohio and 1 from Kentucky. DDC Clinic provided primary medical services to nine of them, three from birth. As part of routine medical care, each patient's detailed medical history and records were collected. Two patients, with the typical phenotype, were clinically diagnosed, but were deceased before their genotype was confirmed, thus their parents' and siblings' genotype were assessed. An additional suspected patient (VIII 4 in Fig. 1), with partial phenotypic expression at birth, expired at 2 days of age and therefore was not included in the phenotype description. Most parents and siblings of the patients also chose to participate in the study. The genealogical information obtained from the affected families



Fig. 2. Clinical characteristics of TMC01 defect syndrome. (A-G) Facial features of the syndrome (low hairline, brachycephaly, flat face, highly arched bushy eyebrows, synophrys, long eyelashes, orbital hyper telorism, wide nose bridge, short nose with antverted nares, microdontism, and generalized gingival hyperplasia) in six patients. Parental consent has been obtained for publication of these photographs. (H) Magnetic resonance imaging (MRI) of brain of a 3 month old female, showing prominence of cerebrospinal fluid (CSF) space around the frontal lobes with extension into the anterior interhemispheric fissure. (I) Chest x ray film of 4 day old male showing multiple rib anomalies.

was confirmed and expanded through the Swiss Anabaptist Genealogical Association (SAGA) group, James C. Hostetler database (<http://www.omii.org>).

Neuropsychological Assessment. A battery of well validated neuropsychological measures, including Wechsler Intelligence Scale WISC R, 1991, was administered to seven affected individuals. To reduce investigator variability and bias, the same clinical psychologist (S.T.) performed the as

essments for each patient in their home environment. Four nonverbal children participated in the study, but the IQ testing results were excluded because of the unreliable results.

Genotyping and Mapping. Total genomic DNA from whole blood was isolated by using the PUREGENE DNA Isolation Kit (Gentra Systems, Minneapolis) according to the manufacturer's protocol. Given the founder effect in iso

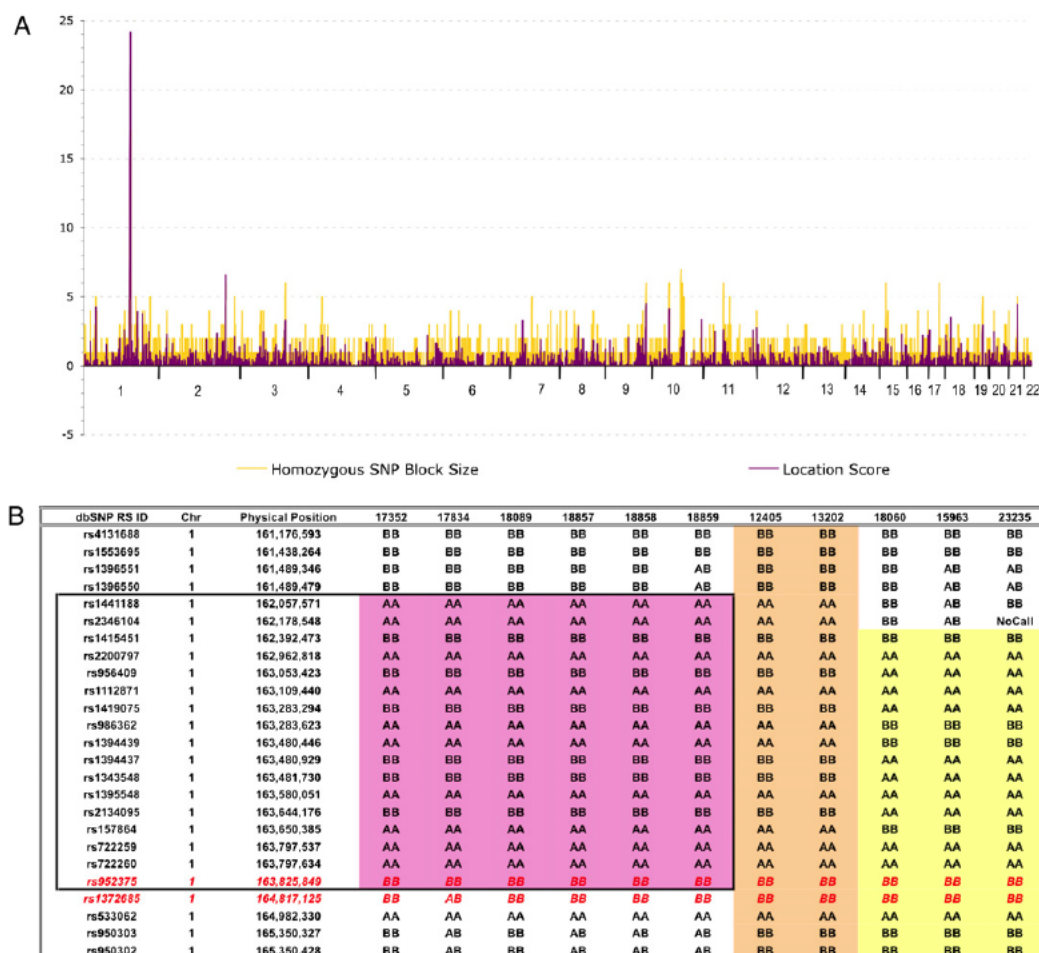


Fig. 3. Genetic mapping of TMC01 defect syndrome found in the Old Order Amish of northeastern Ohio. (A) Autozygosity mapping using Affymetrix GeneChip 10K SNP microarrays and six affected individuals revealed homozygous haplotype identity for 17 SNPs on chromosome 1q23.3 q24.1. (B) Genotypes for 11 affected individuals from 3 separate Amish demes reveal that the TMC01 mutation resides on two distinct SNP haplotypes. The original six patients are displayed first (black box, pink shading). The two Somerset County, PA, patients (next two columns, tan shading) share homozygous haplotype identity with the six original patients, whereas the three Lancaster County, PA, patients are identically homozygous for a distinct haplotype surrounding TMC01 (yellow shading). In all, the 11 genotyped patients share homozygous genotypes at a mere three SNP loci spanning no more than 1.2 Mb. TMC01 physically maps between rs952375 and rs1372685 (red letters).

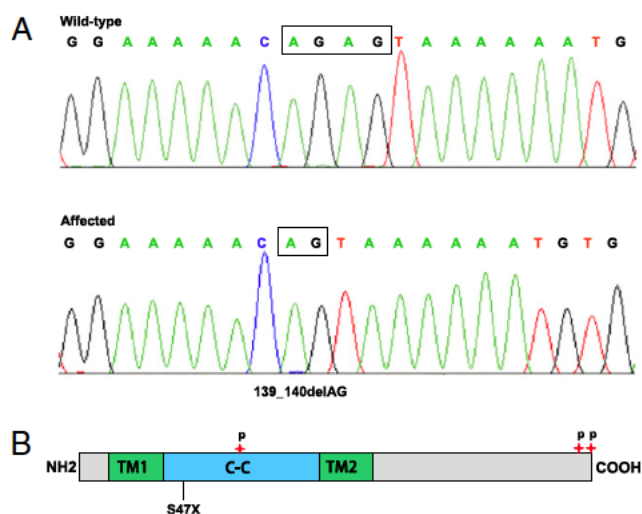


Fig. 4. Identification of the disease causing mutation in *TMCO1* gene. (A) Sequence electropherograms showing the homozygous c.139_140delAG mutation compared with a normal control. (B) Schematic of *TMCO1* protein indicating position of identified mutation and protein structure. Protein structural regions are predicted by SMART. The transmembrane (TM1 and TM2) and coiled coil domains are shown in green and blue, respectively. The three verified phosphoserine residues (S60, S184, and S188) are indicated by red stars.

lated populations such as the Old Order Amish, the disease gene mapping strategy focused on large genomic regions demonstrating homozygosity in all of the affected individuals. DNA samples from six patients were used for genome wide single nucleotide polymorphism (SNP) autozygosity mapping (Fig. 1) by using the Affymetrix GeneChip Mapping 10K assay kit (Affymetrix, Santa Clara, CA) as described in refs. 2 and 3. Genotyping data were analyzed by using customized Excel spreadsheets designed to identify putative autozygous regions of the genome of the affected individuals. SNP positions came from dbSNP build 127 and NCBI build 36 of the human genome. Assuming mutation homogeneity, our analysis examined large, homozygous blocks of SNPs. Population specific SNP allele frequencies were generated from 80 Lancaster County Amish control individuals. Cumulative two point logarithm of odds scores for a block of homozygous SNPs were considered the "location score" for the region. These location scores provided a relative measure of the likelihood that a particular genomic region was autozygous.

1. Raymond FL, Tarpey P (2006) The genetics of mental retardation. *Hum Mol Genet* 15 (Spec No 2):R110–R116.
2. Puffenberger EG, et al. (2004) Mapping of sudden infant death with dysgenesis of the testes syndrome (SIDDT) by a SNP genome scan and identification of TSPYL loss of function. *Proc Natl Acad Sci USA* 101:11689–11694.
3. Strauss KA, et al. (2006) Recessive symptomatic focal epilepsy and mutant contactin-associated protein-like 2. *N Engl J Med* 354:1370–1377.
4. Xin B, Puffenberger EG, Tumbush J, Bockoven JR, Wang H (2007) Homozygosity for a novel splice site mutation in the cardiac myosin-binding protein C gene causes severe neonatal hypertrophic cardiomyopathy. *Am J Med Genet A* 143:2662–2667.
5. Xin B, Puffenberger EG, Nye L, Wiznitzer M, Wang H (2008) A novel mutation in the *GDAP1* gene is associated with autosomal recessive Charcot-Marie-Tooth disease in an Amish family. *Clin Genet* 74:274–278.

Mutation Identification. PCR primers were designed to amplify each of the seven protein coding exons and their flanking intronic sequences of *TMCO1*. We designed primer sequences (Table S1) by using Primer3 software (<http://frodo.wi.mit.edu/primer3>). PCR amplifications were performed by using 50 ng of genomic DNA in each reaction. The PCR products were examined on 1% agarose gels and purified for sequencing by using Qiaquick spin columns (QIAGEN, Valencia, CA). Sequencing reactions were performed by using the Big Dye terminator v3.1 cycle sequencing kit (Applied Biosystems, Foster City, CA), and the extension products were analyzed on an Applied Biosystems 310 Genetic Analyzer. The identified mutation was verified with repeat PCR amplification and sequencing in both orientations. Sample sequences were compared to the GenBank reference sequences by using Mutation Surveyor software (SoftGenetics LLC, State College, PA) for identification of sequence variants. The GenBank accession numbers of both genomic DNA and mRNA reference sequences used in this study are NT 004487 and NM 019026, respectively. We performed protein domain analysis by using the Simple Modular Architecture Research Tool (SMART; <http://smart.embl-heidelberg.de>). We generated amino acid sequence alignments of *TMCO1* orthologs by the ClustalW2 program (www.ebi.ac.uk/Tools/clustalw2/index.html).

cDNA Amplification. PCR amplification of *TMCO1* cDNA was performed by using primers F117 and R462 located in exons 1 and 6 (Table S1, the base pair numbers of primers were determined according to the mRNA sequence NM 019026). The tissue distribution of *TMCO1* transcript was determined by RT-PCR. Both adult and fetal human multiple tissue cDNA (MTC) panels were obtained commercially (Clontech, Mountain View, CA). PCR amplification of *TMCO1* and *GAPDH* (positive control) sequences were performed according to the manufacturer's protocol. Thirty PCR cycles for *TMCO1* and twenty four cycles for *GAPDH* were performed. The PCR products were then electrophoresed on a 1.5% agarose gel.

ACKNOWLEDGMENTS. We thank the families for their patience and support. We appreciate the many physicians who provided outstanding and compassionate care to the children affected by the disease, particularly Dr. John Tumbush in Middlefield and many others from Akron Children's Hospital, Rainbow Babies and Children's Hospital, and Shriners Hospitals for Children. We are indebted to Dr. Irvin Schafer and Dr. Kurt Wegner, who helped us evaluate three patients; Dr. Guiyun Wu, who helped us review and interpret imaging studies; and Miss Carol Troyer, who helped with the data collection. We acknowledge Drs. Holmes Morton and Kevin Strauss for their continuous support throughout the project, their valuable contributions in the evaluation of patients at the Clinic for Special Children, critical reading, and suggestions to the manuscript. The study was supported in part by The Elisabeth Severance Prentiss Foundation, The Reinberger Foundation, and the Leonard Krieger Fund of the Cleveland Foundation (L2009 0078).

6. Strauss KA, Puffenberger EG (2009) Genetics, medicine, and the Plain people. *Annu Rev Genomics Hum Genet* 10:513–536.
7. Olsen JV, et al. (2006) Global, in vivo, and site-specific phosphorylation dynamics in signaling networks. *Cell* 127:635–648.
8. Nousiainen M, Silljé HHW, Sauer G, Nigg EA, Körner R (2006) Phosphoproteome analysis of the human mitotic spindle. *Proc Natl Acad Sci USA* 103:5391–5396.
9. Daub H, et al. (2008) Kinase-selective enrichment enables quantitative phosphoproteomics of the kinome across the cell cycle. *Mol Cell* 31:438–448.
10. Dephourse N, et al. (2008) A quantitative atlas of mitotic phosphorylation. *Proc Natl Acad Sci USA* 105:10762–10767.
11. Iwamuro S, Saeki M, Kato S (1999) Multi-ubiquitination of a nascent membrane protein produced in a rabbit reticulocyte lysate. *J Biochem* 126:48–53.
12. Zhang Z, et al. (2009) Molecular cloning, expression patterns and subcellular localization of porcine *TMCO1* gene. *Mol Biol Rep*, in press.